

000 001 002 003 004 005 DETECTING DISTILLATION DATA FROM REASONING 006 MODELS 007 008 009

010 **Anonymous authors**
011 Paper under double-blind review
012
013
014
015
016
017
018
019
020
021
022
023
024
025

ABSTRACT

026 Reasoning distillation has emerged as an efficient and powerful paradigm for
027 enhancing the reasoning capabilities of large language models. However, reasoning
028 distillation may inadvertently cause benchmark contamination, where evaluation
029 data included in distillation datasets can inflate performance metrics of
030 distilled models. In this work, we formally define the task of **distillation data**
031 **detection**, which is uniquely challenging due to the partial availability of distil-
032 lation data. Then, we propose a novel and effective method *Token Probability*
033 *Deviation (TBD)*, which leverages the probability patterns of the generated *out-
034 put* tokens. Our method is motivated by the analysis that distilled models tend to
035 generate near-deterministic tokens for seen questions, while producing more low-
036 probability tokens for unseen questions. Our key idea behind TBD is to quantify
037 how far the generated tokens' probabilities deviate from a high reference probabili-
038 ty. In effect, our method achieves competitive detection performance by produc-
039 ing lower scores for seen questions than for unseen questions. Extensive exper-
040 iments demonstrate the effectiveness of our method, achieving an AUC of **0.918**
041 and a TPR@1% FPR of **0.470** on the S1 dataset.
042
043

1 INTRODUCTION

044 Large Reasoning Models (LRMs) have shown impressive performance on complex tasks like mathematical reasoning and coding problems (Jaech et al., 2024; Guo et al., 2025; Yang et al., 2025; xAI, 2025). By articulating intermediate steps via Chain-of-Thought (CoT), LRMs dynamically allocate extra compute to challenging problems. However, such reasoning capabilities are typically limited to LRMs exceeding 100 billion parameters, hindering practical deployment in resource-constrained settings (Wei et al., 2022). To address this, recent studies have explored reasoning distillation, transferring reasoning abilities from LRMs to Small Language Models (SLMs) by simulating reasoning traces (Chen et al., 2025; Ye et al., 2025; Muennighoff et al., 2025b; Liu et al., 2025). This paradigm has been widely applied in cutting-edge models, such as DeepSeek R1 series (Guo et al., 2025), Sky-T1-32B-preview (Team, 2025), and Bespoke-32B (Labs, 2025).

045 In reasoning distillation, current methods generate reasoning trajectories and answers from LRMs
046 for domain-specific questions, using these to supervise SLM training (Wu et al., 2025b; Li et al.,
047 2025). Yet, the lack of transparency regarding distillation data raises concerns about benchmark
048 contamination, where evaluation data inadvertently included in training can inflate performance
049 metrics (Oren et al., 2024a; Xu et al., 2024a). These issues highlight the need to detect distillation data
050 for distilled SLMs, ensuring transparency and fairness. Different from training data detection (Shi
051 et al., 2024; Zhang et al., 2025b), the unique challenge of this task lies in partial availability: only
052 the question is available at detection, without access to corresponding reasoning trajectories and
053 answers. Accessing question-response pairs is generally infeasible due to the non-deterministic
054 generation process in solution construction (Ye et al., 2025; Wu et al., 2025a) and the proprietary
055 nature of datasets (Guo et al., 2025; Yang et al., 2025). Consequently, existing methods operating
056 on input sequences struggle to obtain reliable membership signals given partial sample information.

057 In this study, we demonstrate that tokens generated by distilled models can expose information
058 for identifying their distillation data. We observe that distilled models generally exhibit different
059 probability distributions for members (*i.e.*, seen questions) and non-members (*i.e.*, unseen questions)
060 in greedy decoding. In particular, distilled models tend to generate near-deterministic tokens for

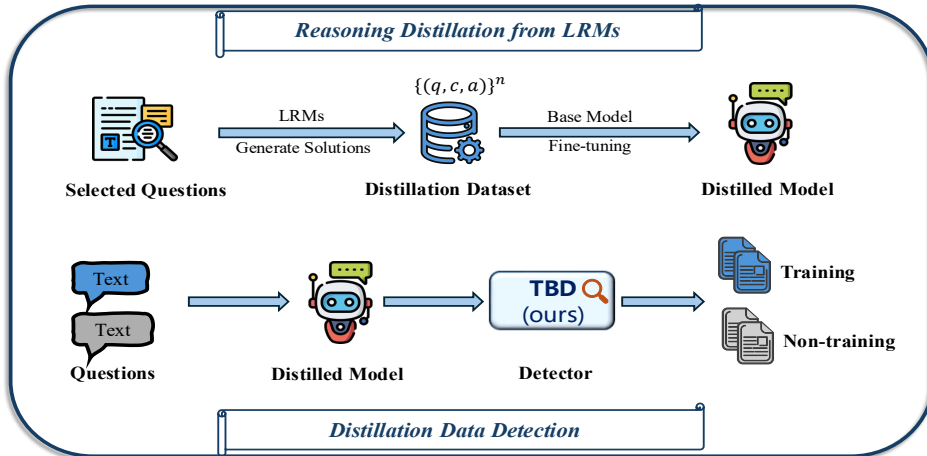


Figure 1: **Overview of distillation data detection.** The top panel illustrates the pipeline of the reasoning distillation that distils the reasoning capacities of LRM to smaller LLMs. The bottom panel illustrates the process of detecting distillation data.

members, while producing more low-probability tokens for non-members. This difference in token generation behavior indicates that the probability distributions of distilled models can be used to determine whether a given question was seen in the distillation process.

Inspired by the analysis, we propose a simple yet effective method – [Token Probability Deviation \(dubbed TBD¹\)](#), which detects the distillation data through the probabilities of generated tokens, instead of input tokens. Our key idea behind TBD is to quantify how far the probabilities of generated tokens are from being fully deterministic. In particular, this can be accomplished by measuring the deviation of the generated token’s probability from a high reference probability. In effect, our method produces smaller scores for members than for non-members at test time. By way of our method, we can achieve a clear separability of scores between seen and unseen questions, even when only the question component of each sample is available.

Empirically, we perform extensive experiments to validate the effectiveness of the proposed method across diverse models and various datasets, including S1, S1.1 ([Muennighoff et al., 2025a](#)) and LIMO ([Ye et al., 2025](#)). The results demonstrate that our method can significantly achieve superior performance than existing methods for detecting distillation data (See Table 1). For example, our method achieves an AUC of 0.918 and a TPR@1%FPR of 0.470 on the distilled model obtained by fine-tuning Qwen2.5-32B-Instruct on the S1 dataset, indicating the effectiveness of our method for detecting distillation data. Moreover, the ablation study shows that components in our method contribute to the overall high performance. In addition, experimental results show the robustness of our method across various datasets and models, enabling us to deploy our algorithm without task-specific hyperparameter tuning. In summary, our method shows superior performance in both the AUC and TPR@1%FPR metrics, showing the practicality of our method in real-world applications.

Our contributions and findings are summarized as follows:

- We first present the problem of distillation data detection and emphasize its unique challenge of partial availability. We then analyze the limitations of existing methods in the task of detecting distillation data.
- We propose Token Probability Deviation (dubbed **TBD**), a novel and effective method for detecting distillation data. The core idea of our method is to measure the deviation of generated tokens’ probabilities from a high reference probability.
- We empirically show that our method can significantly outperform baselines for detecting distillation data, through extensive experiments conducted on various models and datasets.

¹We denote the probability by B in our method, referred to as TBD.

108

2 PRELIMINARIES

110 **Reasoning distillation.** Reasoning distillation transfers the step-by-step reasoning behavior of
 111 large reasoning models (LRMs) into a smaller student language model by imitating the reasoning
 112 trajectories generated by teacher models (Guo et al., 2025; Li et al., 2025). Let q denote a
 113 question drawn from a large-scale corpus \mathcal{Q} , collected from diverse sources. Using q as a prompt,
 114 developers usually use LRMs to generate reasoning trajectories c along with the final answer a (See
 115 Appendix B.1 for an example). To construct a high-quality distillation dataset $\mathcal{D} = \{(q_i, c_i, a_i)\}_{i=1}^N$,
 116 developers then execute a meticulous selection process from an initial large-scale pool of candidates.
 117 The goal of reasoning distillation is to obtain a distilled model by fine-tuning an SLM on the result-
 118 ing distillation dataset (See Figure 1). Formally, the objective of training can be formulated as:

$$119 \quad \mathcal{L}_\theta = \sum_{t=1}^N \log P_\theta(y_t | y_{<t}, q), \quad (1)$$

120 where q denotes the input question, and $y = \{y_1, y_2, \dots, y_N\}$ represents the corresponding target
 121 sequence, comprising the reasoning trajectory c and the final answer a . $P_\theta(y_t | y_{<t}, q)$ denotes the
 122 predicted probability of model for token y_t , given preceding tokens. This paradigm explicitly trains
 123 the student model to reproduce intermediate reasoning, aiming to internalize not just the outcomes
 124 but the procedural patterns of teacher models.

125 **Membership inference.** Membership Inference Attacks (MIAs) aim to predict whether a partic-
 126 ular record is included in the training data (Shokri et al., 2017). MIAs are often used as a measure
 127 of information leakage, such as privacy disclosure (Mozes et al., 2023), copyright violations (Chang
 128 et al., 2023), and test set contamination (Xu et al., 2024a; Choi et al., 2025). The definition of
 129 *traditional MIAs* is as follows: Given a trained model $f(\mathbf{x}, \theta)$ and a data point (\mathbf{x}, y) , an attacker
 130 infers whether a target data point belongs to the training data \mathcal{D}_{train} . In traditional MIA settings,
 131 they often require strong assumptions, such as training multiple shadow models and accessing to the
 132 underlying data distribution. This is often impractical for LLMs due to the unavailability of training
 133 data distribution and high training costs. The existing MIAs on LLMs usually aim to determine
 134 whether a given piece of text \mathbf{x} is part of the training dataset for a large language model \mathcal{M} , by
 135 computing a membership score $S(\mathbf{x}, \mathcal{M})$. Training data detection methods for LLMs generally de-
 136 sign a scoring function that computes a score for each input (Li, 2023; Shi et al., 2024; Zhang et al.,
 137 2025b). Although some methods for pretraining and fine-tuning data detection have been studied,
 138 membership inference on distillation data for reasoning distillation remains underexplored. In the
 139 next section, we introduce the distillation data detection task, a tailored formulation of this problem.

140

3 DISTILLATION DATA DETECTION

141 In this section, we formally define the ***Distillation Data Detection*** task, which is uniquely challeng-
 142 ing due to the partial availability of distillation data. The goal of our task is to predict whether a
 143 given question is included in the model’s distillation dataset.

144 **Problem definition.** Using question q as a prompt, developers often generate training data by
 145 sampling responses from multiple advanced LRMs and by refining them to obtain high-quality rea-
 146 soning trajectories c and corresponding answer a (Ye et al., 2025; Wu et al., 2025b; Tian et al.,
 147 2025; Zhuang et al., 2025). However, the resulting distillation dataset $\mathcal{D} = \{(q_i, c_i, a_i)\}_{i=1}^N$ is often
 148 proprietary (Guo et al., 2025; Yang et al., 2025)—i.e., the exact reasoning trajectory and answer are
 149 inaccessible for a given question. Also, due to the non-deterministic generation process and post-
 150 hoc filtering, it is generally infeasible to recover the exact reasoning trajectory or answer associated
 151 with a given question. Thus, we study a more practical *question-only* setting in which an auditor
 152 can query a distilled model \mathcal{M} with question q and obtain model outputs, but has no access to the
 153 corresponding reasoning trajectories c and answer a of a datapoint.

154 Formally, let $\mathcal{Q}_{\mathcal{D}} = \{q_i : (q_i, c_i, a_i) \in \mathcal{D}\}$ denote the set of questions from a distillation dataset
 155 used for training base models. We pose distillation data detection as a level-set estimation problem
 156 defined on a scoring function $S(q, \mathcal{M})$ as:

$$157 \quad G(q; \mathcal{M}) = \begin{cases} 1 & \text{if } S(q, \mathcal{M}) < \lambda, \\ 0 & \text{if } S(q, \mathcal{M}) \geq \lambda, \end{cases} \quad (2)$$

162 where $G = 1$ indicates *member* ($q \in \mathcal{Q}_D$) and $G = 0$ indicates *non-member* ($q \notin \mathcal{Q}_D$), with λ being
 163 a case-dependent threshold. The key difficulty of this task lies in **partial availability**: the training
 164 datapoint is triple $x = (q, c, a)$, yet only the question q is available at test time. Consequently, the
 165 design of \mathcal{S} must rely solely on question-conditioned behaviours of \mathcal{M} , rather than on likelihood-
 166 driven metrics over the ground truth (c, a) .
 167

168 **Challenge of partial availability.** Most prior work on training data detection for LLMs assumes
 169 access to the *entire* training sample, which contains complete information seen during training (Mat-
 170 tern et al., 2023; Fu et al., 2024; Mireshghallah et al., 2022). In this setting, the scoring function
 171 \mathcal{S} can be defined directly in terms of sample likelihoods, exploiting probability estimates over in-
 172 put tokens. Existing training data detection approaches targeting LLMs typically leverage a scoring
 173 function that computes a score for each input sequence. For example, MIN-K% (Shi et al., 2024)
 174 computes the average log-likelihood of the lowest K% tokens scores over the input, effectively using
 175 low-probability tokens as signals of membership. Such approaches are well-suited when full sample
 176 information is observable at detection time.
 177

178 However, these approaches may perform poorly in the
 179 setting of distillation data detection, where distillation
 180 data are only partially available. The absence of joint
 181 question-response pairs weakens the key signal exploited
 182 by likelihood-based approaches operating over input se-
 183 quences, leaving them ill-suited for this task. To illustrate,
 184 we analyze the distribution of MIN-K% scores for mem-
 185 ber versus non-member questions. As shown in Figure 2,
 186 the two distributions exhibit substantial overlap, indicat-
 187 ing limited separability and poor discriminative power
 188 when only questions are available. This highlights the
 189 requirement for alternative scoring functions effective un-
 190 der partial availability. Motivated by the challenge of par-
 191 tial availability, we investigate whether the *token genera-
 192 tion behavior* of distilled models, conditioned solely on
 193 q , can serve as a reliable signal of membership.
 194

4 METHOD

195 To address the challenge of partial availability, we explore a question-only scoring approach that
 196 leverages the token-level generation behavior of distilled reasoning models. We begin by comparing
 197 the probability patterns of tokens between member and non-member questions (See Section 4.1).
 198 Then, building on our empirical observations, we propose *Token Probability Deviation* (TBD), a
 199 simple yet effective method to detect distillation data (See Section 4.2).
 200

4.1 MOTIVATING ANALYSIS

201 **Analysis setup.** The goal of our analysis is to investigate whether the token-level probability pat-
 202 terns produced by a distilled model differ between member and non-member questions. Following
 203 prior work (Muennighoff et al., 2025b), we first distill the reasoning capabilities to the Qwen2.5-
 204 32B-Instruct model via supervised full-parameter fine-tuning on the S1 dataset. The dataset is split
 205 into training and testing subsets with an 8:2 ratio, from which we sample members (training set)
 206 and non-members (testing set). This ensures an i.i.d setup, with both groups drawn from the same
 207 underlying data distribution. For each question, we generate a response from the distilled model
 208 using greedy decoding and extract the token probabilities of the response for comparison. Example
 209 question prompts are provided in Appendix B.2.
 210

211 **Members generate near-deterministic tokens more frequently.** To examine distributional dif-
 212 ferences in token probabilities, we analyze sequences of up to 300 generated tokens for both mem-
 213 ber and non-member questions. Figure 3a shows the token-wise maximum probability distributions
 214 from the distilled model across 20 member and 20 non-member samples. The horizontal axis de-
 215 notes the token index, while the vertical axis reports the probability assigned to the corresponding
 216

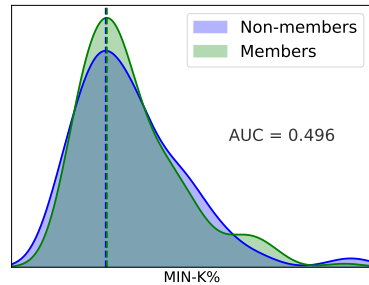


Figure 2: Scores distribution of MIN-K% for members and non-members, obtained from the distilled model trained on the LIMO dataset using the Qwen2.5-32B-Instruct base model.

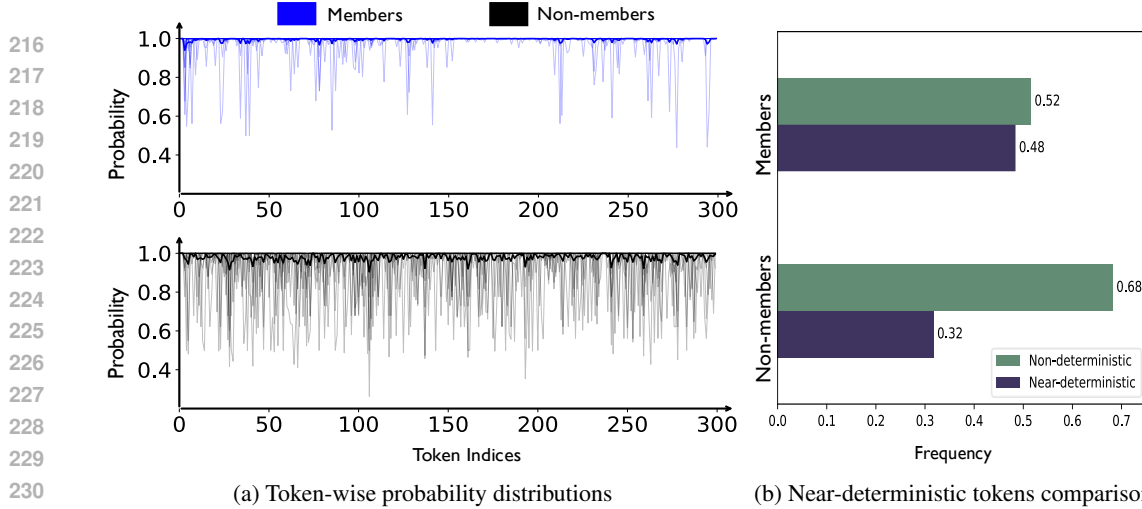


Figure 3: Comparison of token-level generation behaviour of distilled models for 20 member and 20 non-member questions under greedy decoding. **(a) Token-wise probability distributions:** we contrast the distribution of token-wise probability between members and non-members, showing that non-members tend to produce more tokens with lower probability. **(b) Near-deterministic vs. non-deterministic tokens:** near-deterministic tokens denote generated tokens with probabilities approaching 1, and vice versa for non-deterministic tokens. The distilled reasoning model tends to generate more near-deterministic tokens for members.

token. Thin lines correspond to individual samples, and bold lines denote mean token-wise probability across all members or non-members. We observe that the distilled model tends to frequently generate tokens with probabilities close to 1 for members, while producing more low-probability tokens for non-members. Figure 3b further contrasts the frequency of near-deterministic tokens (with probability approaching 1) against non-deterministic tokens. The results show that the distilled model produces a substantially higher fraction of near-deterministic tokens for member questions. This suggests that generation probabilities are likely to carry membership signals, motivating our design of a scoring function that leverages tokens generated by the distilled model to detect distillation data. Building on these insights, we introduce *Token Probability Deviation* in the next section.

4.2 TOKEN PROBABILITY DEVIATION

Motivated by our preliminary analysis, we propose Token Probability Deviation (TBD), a method that exploits the observation that member questions tend to elicit near-deterministic tokens, whereas non-members induce relatively more low-probability tokens. Unlike many methods for detecting training data from LLMs, which rely on *input* token probabilities (Shi et al., 2024; Zhang et al., 2025b), TBD utilizes the *generated* token probabilities along the model’s reasoning trajectory for given question q . This design sidesteps the partial-availability constraint of distillation datasets while providing a simple, model-agnostic signal for distillation data detection.

Token Probability Deviation. The core idea of our method is to measure the deviation of the generated tokens’ probability from a high reference probability. Given a question entailed with a sequence of tokens $q = \{q_1, q_2, \dots, q_N\}$, the tokens generated by model can be denoted as $y = \{y_1, y_2, \dots, y_i\}$. We use $p_\theta(y_i \mid y_{<i}, q)$ to denote the probability that the target model predicts y_i , given the question prompt q and the generated text prefix $y_{<i} = \{y_1, y_2, \dots, y_{i-1}\}$. We first quantify the deviation between the probability of the generated token y_i and the reference probability τ . Formally, we define the deviation term as:

$$d_i(q; \tau) = \max(0, \tau - p_\theta(y_i \mid y_{<i}, q)), \quad (3)$$

where $\max(0, \cdot)$ ensures that only outlier tokens, whose probabilities are below the threshold τ , contribute to the final score computation. Since distilled reasoning models tend to generate tokens with extremely high probability for seen questions, outlier tokens are likely to display a highly

270 distinctive membership signal. Therefore, by computing the deviation of the outlier tokens, we
 271 expect to obtain a more distinctive signal for data membership.
 272

273 Considering that the earlier generated tokens are likely to be more representative of the behaviour
 274 of the model for members and non-members, we perform a truncation operation to focus on the first
 275 M generated tokens. To obtain the final robust sentence-level score, we compute the average of the
 276 token’s deviation $d_i(q; \tau)$. Concretely, the final score can be formulated as:
 277

$$\mathcal{S}(q, \theta) = \frac{1}{E} \sum_{i=1}^M d_i(q; \tau)^\alpha, \quad (4)$$

280 where $E = \sum_{i=1}^M \mathbf{1}(p_\theta(y_i | y_{<i}, q) < \tau)$ denotes the number of outliers among the first M tokens.
 281

282 In practice, we introduce a tunable parameter α to adjust the contribution of tokens to the scoring
 283 function. For instance, a small value of α (e.g., 0.6) can amplify the deviation of a generated token’s
 284 probability from τ . Our experimental results in Figure 4b show that a suitable α can yield an
 285 improved TPR@1% FPR for detecting distillation data.
 286

287 **Detection with token probability deviation.** Our method enables us to build a detector $G(q; M)$
 288 for a distilled reasoning model to infer the membership of question q . In particular, our method is
 289 robust across various datasets, enabling us to deploy our algorithm without task-specific hyperpa-
 290 rameter tuning. At test time, samples with lower scores $\mathcal{S}(q, \theta)$ are classified as distillation data and
 291 vice versa. By way of our method, we can obtain a clear distinction between seen questions and
 292 unseen questions, establishing excellent performance for detecting distillation data.
 293

5 EXPERIMENTS

295 In this section, we evaluate the performance of our method across several datasets with multiple
 296 models of different sizes. Extensive experiments demonstrate the effectiveness of our method, which
 297 designs a scoring function using generated tokens instead of input tokens.
 298

5.1 EXPERIMENTAL SETUP

300 **Datasets and models.** We conduct experiments on several high-quality distillation datasets pro-
 301 vided by previous work, including S1, S1.1 (Muennighoff et al., 2025b) and LIMO (Ye et al., 2025).
 302 The details of datasets are provided in Appendix B.1. Specifically, we fine-tune the base model (e.g.,
 303 Qwen2.5-32B-Instruct) on these datasets with a full-parameter supervised fine-tuning strategy. In
 304 addition, we also perform experiments on different-sized base models, such as Qwen2.5-7B-Instruct,
 305 Qwen2.5-14B-Instruct and Qwen2.5-32B-Instruct models (Qwen et al., 2025).
 306

307 **Baseline methods.** We compare our method with current competitive baselines: (1) **Perplex-
 308 ity** (Li, 2023): uses the perplexity of input text as a metric. (2) **Zlib** (Carlini et al., 2021): computes
 309 the ratio of example perplexity and zlib compression entropy (3) **Lowercase** (Carlini et al., 2021):
 310 computes the ratio of the perplexity on the text before and after lowercasing. (4) **Neighbor** (Mat-
 311 tern et al., 2023): perturbs the input sentence with masked language models to create “neighbor”
 312 and compares the loss of the input sentence with the average loss of the neighbor sentences. (5)
 313 **Min-K%** (Shi et al., 2024): computes the average log-likelihood of K% outlier tokens with the
 314 smallest predicted probability. (6) **Min-K%++** (Zhang et al., 2025b): compares the probability
 315 of the target token with the expected probability of all tokens within the vocabulary. (7) **Infilling
 316 Score** (Raoof et al., 2025): computes the ratio of the infilling probability of the ground-truth token
 317 and the maximum causal likelihood token. These methods typically detect training data by design-
 318 ing likelihood-based scores derived from input tokens, while our method leverages tokens generated
 319 from models to detect training data. Additionally, we introduce two vanilla variants of our method,
 320 which use generated tokens to determine data membership. Specifically, (8) **Generated Perplex-
 321 ity**: computes the perplexity using the probabilities of generated tokens. (9) **Generated Min-K%:**
 322 computes the average log-likelihood of K% generated tokens with the lowest predicted probability.
 323

Implementation details. To effectively evaluate our method, we fine-tune the Qwen2.5-32B-
 324 Instruct model separately on S1, S1.1, and LIMO distillation datasets to obtain diverse distilled
 325

Table 1: AUC of our method and baselines on diverse distilled models. These models are produced through fine-tuning diverse different-sized models (e.g., Qwen2.5-32B-Instruct) on various distillation datasets, including S1, LIMO and S1.1 datasets. \dagger indicates methods that compute score using output tokens. **Bold** shows the superior result.

Method	Qwen2.5-7B-Instruct			Qwen2.5-14B-Instruct			Qwen2.5-32B-Instruct		
	S1	LIMO	S1.1	S1	LIMO	S1.1	S1	LIMO	S1.1
<i>Input-token-based methods</i>									
Perplexity (Li, 2023)	0.444	0.482	0.503	0.449	0.498	0.517	0.433	0.499	0.487
Lowercase (Carlini et al., 2021)	0.435	0.472	0.493	0.467	0.507	0.489	0.459	0.475	0.463
Zlib (Carlini et al., 2021)	0.474	0.486	0.467	0.467	0.495	0.471	0.448	0.496	0.447
Neighbor (Mattern et al., 2023)	0.539	0.503	0.441	0.543	0.500	0.435	0.555	0.503	0.444
MIN-K% (Shi et al., 2024)	0.443	0.480	0.494	0.453	0.496	0.509	0.437	0.496	0.479
MIN-K%++ (Zhang et al., 2025b)	0.472	0.458	0.486	0.509	0.508	0.489	0.461	0.461	0.439
Infilling Score (Raoof et al., 2025)	0.529	0.529	0.520	0.534	0.544	0.493	0.574	0.489	0.475
<i>Output-token-based methods</i>									
Generated Perplexity \dagger	0.753	0.605	0.564	0.785	0.596	0.558	0.847	0.662	0.619
Generated MIN-K \dagger	0.754	0.604	0.563	0.785	0.596	0.559	0.847	0.661	0.619
Ours \dagger	0.855	0.694	0.617	0.870	0.671	0.562	0.918	0.728	0.649

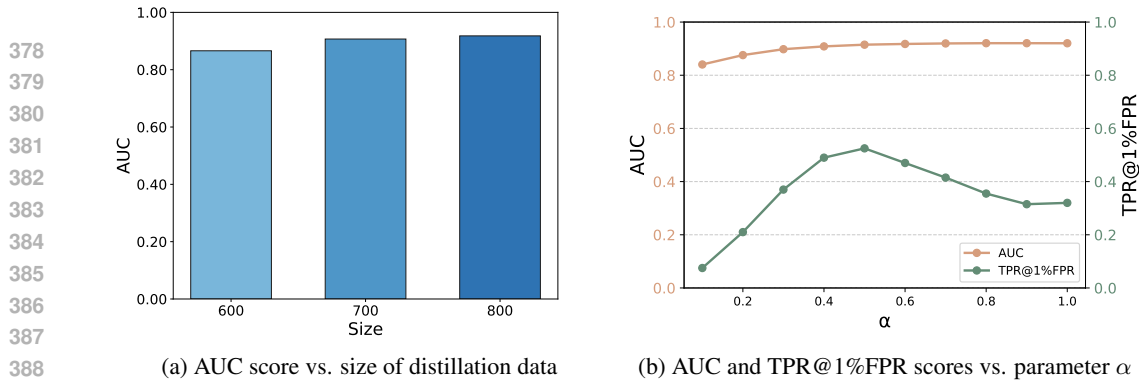
reasoning models. For the main results, the original datasets are split into training and testing subsets, with an 8:2 train-test split. We then perform full-parameter fine-tuning on 8 A100 GPUs using DeepSpeed ZeRO-3 optimization, with a sequence length limit of 16,384 tokens. The details of training parameters are provided in the Appendix B.2. To ensure fair evaluation, we construct balanced datasets of member and non-member samples, drawn respectively from the training and test sets, ensuring an IID setting. For two vanilla variants of our method, *Generated Perplexity* and *Generated Min-K%*, the sample score is computed using only the first 1,000 generated tokens. For main experiments, we apply a greedy decoding strategy for generation, and compute the TBD score using the first 300 generated tokens with $\tau = 1$ and $\alpha = 0.6$.

Evaluation metrics. We evaluate the performance of our method and baselines for detecting distillation data by measuring the following metrics: (1) AUC, the area under the receiver operating characteristic curve; (2) TPR@1%FPR, the true positive rate at 1% false positive rate (Carlini et al., 2022). Instead of paying equal attention to members and nonmembers, this metric pays more attention to members and evaluates whether one can confidently identify members.

5.2 EXPERIMENTAL RESULTS

Is our method effective across models trained on various datasets? To investigate the performance of our method across diverse distilled reasoning models, we fine-tune the diverse models on three distillation datasets, including S1, LIMO and S1.1 datasets. Table 1 shows that our method significantly outperforms the baselines, achieving superior performance for detecting distillation data. We also present the TPR@1% FPR score of our method and baselines in Appendix C.2. Firstly, our experiments demonstrate that tokens generated by distilled models can serve as effective information for detecting distillation data. Furthermore, empirical evidence suggests that our method can detect distillation data even under a low false-positive rate constraint, showing the practicality of our method in real-world applications. For example, our method achieves a high AUC of 0.918 and a TPR@1% FPR of 0.470 on the distilled model obtained by fine-tuning Qwen2.5-32B-Instruct on S1. Overall, our experimental results demonstrate the effectiveness of our method for detecting distillation data across diverse models and datasets.

Is our method effective across various models? To investigate the effectiveness of our method across various models, we conduct experiments on the S1 dataset with three different LLMs, including Llama-3.1-8B-Instruct (Dubey et al., 2024), Gemma-7B-it (Team et al., 2024) and Mistral-7B-Instruct-v0.3 (Jiang et al., 2023) models. In Appendix C.2, we provide the AUC and TPR@1%FPR scores for our method and the baselines across various models. The results indicate that our method

Figure 4: Effect of distillation data size (4a) and parameter α (4b) on our method’s performance.

consistently achieves superior performance compared to baselines, demonstrating its model-agnostic nature and broad applicability.

Is our method effective with models of different parameter sizes? To validate the effectiveness of our methods on distilled models of different sizes, we fine-tune Qwen2.5-7B-Instruct, Qwen2.5-14B-Instruct, and Qwen2.5-32B-Instruct models on various datasets, respectively. As presented in Table 1, the results show that our method achieves superior performance for detecting distillation data, demonstrating the effectiveness of our method across models of different sizes. **Among three models of different sizes, our method achieves the best AUC and TPR@1%FPR on the S1 dataset under the 32B model.** The properties of models and characteristics of datasets may potentially influence our method’s performance.

How does the distillation data size affect our method? To investigate the performance of our method on varying dataset scales, we conduct experiments on the S1 dataset and fine-tune Qwen2.5-32B-Instruct with data sizes of 600, 700, and 800. At test time, we construct a balanced dataset to evaluate the performance of our method. Figure 4a shows the AUC of our method with various sizes of distillation datasets. The results demonstrate our method consistently achieves reliable detection performance across diverse distilled models. In addition, we observe that the AUC of our method slightly increases with the size of the distillation dataset, likely because the distilled model trained on more data exhibits enhanced generation behaviour that improves detection. In summary, our experiment indicates the effectiveness of our method with distillation datasets of different sizes.

How does α affect the performance of our method? Our method introduces a tunable parameter α to adjust the contribution of tokens on the sample score. For instance, a small value of α amplifies the deviation of a generated token’s probability from τ , thereby increasing its impact on the sample score when deviations are minor. We conduct experiments with varying α values to examine their effect on our method’s performance, based on the distilled model fine-tuned from Qwen2.5-32B-Instruct on S1. Figure 4b shows the AUC and TPR@1%FPR scores of our method with varying α . Note that setting α to 1 is equivalent to applying our method without deviation adjustment. Increasing α initially improves the AUC score, and performance ultimately stabilizes as α continues to increase. The TPR@1%FPR score significantly rises as α increases, reaching a peak near $\alpha = 0.6$, and subsequently decreases. This behaviour allows us to deploy our algorithm flexibly by simply adjusting α , targeting the preferred metric in practical applications. Overall, our method can significantly improve TPR@1%FPR by applying a α in our method.

How does truncation length M affect the performance of our method? Our method introduces a truncation operation to compute the sample score using the first M generated tokens. To study how the length of tokens affects the performance of our method, we perform an evaluation by adjusting the number of tokens used to compute the score. Concretely, we set the number of tokens from 50 to 1000 with a step size of 50. In our experiment, setting the truncation length to 300 corresponds to computing the score using the first 300 generated tokens. We evaluate our method on distilled models obtained by fine-tuning Qwen2.5-32B-Instruct on three distillation datasets, reporting the AUC and TPR@1%FPR of our method with different truncation lengths. The figure 5a shows that

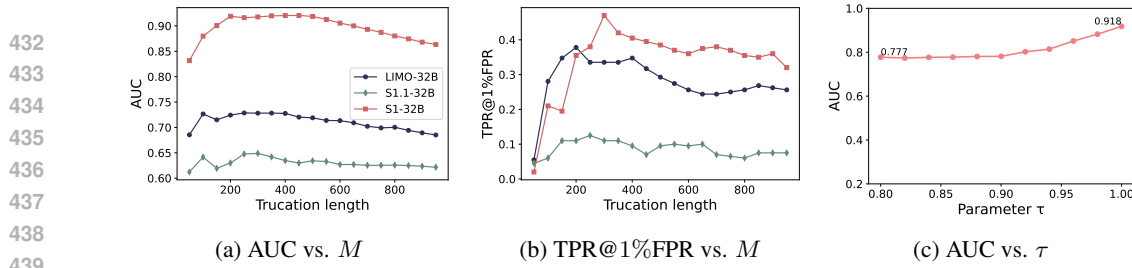


Figure 5: Ablation study on hyperparameter M and threshold τ . We present AUC and TPR@1%FPR of our method with varying truncation length M on three datasets (5a & 5b), and AUC of our method under varying threshold τ on the S1 dataset (5c).

Table 2: Ablation study on the components of our method with the distilled model fine-tuned from Qwen2.5-32B-Instruct on the S1 dataset. Note that excluding parameter α corresponds to setting $\alpha = 1$. The grey rows correspond to the final design of our method with different α . **Bold** shows the superior result, with the runner-up underlined.

Truncation length	Token deviation	Parameter α	AUC	TPR@1% FPR
\times	\times	\times	0.847	0.170
$M = 300$	\times	\times	0.903	0.290
$M = 300$	\checkmark	\times	0.920	0.320
$M = 300$	\checkmark	$\alpha = 0.6$	<u>0.918</u>	0.470
$M = 300$	\checkmark	$\alpha = 0.7$	0.920	<u>0.415</u>

the AUC initially increases with truncation length, but declines as the length continues to increase. Our method consistently reaches its optimal performance across various datasets when the truncation length is around 300. Similarly, Figure 5b show that the TPR@1%FPR score exhibits a similar trend. These findings indicate the robustness of our method across various datasets, allowing users to deploy our algorithm with a fixed truncation length value.

Effect of threshold τ on the performance of our method. Our method introduces a reference probability τ to quantify the deviation of the generated token’s probability from the reference probability. In Figure 5c, we show the AUC of our method with varying τ on the distilled model obtained by fine-tuning Qwen2.5-32B-Instruct on S1. The result shows that our method achieves superior performance with a large value of τ . As described in Section 4.1, the distilled reasoning model tends to generate tokens with extremely high probability. Thus, applying a high reference probability can help identify outlier tokens and achieve better performance for detecting distillation data.

Decomposing the contribution of our method. As described in Equation 4, our method can be decomposed into three key components: (1) truncation operation M , which truncates the generated sequence to the first M tokens; (2) token deviation measure $d_i(q; \tau)$, which measures the deviation of the generated token’s probability from a reference probability τ ; and (3) tunable parameter α , which adjusts the contribution of tokens on the sample score. To elucidate individual contributions of each component, we conduct an ablation study in Table 2. We start by computing the average predicted probabilities over the first 1000 generated tokens. We then gradually incorporate the truncation operation, token deviation measure, and parameter α into the score computation, leading to the final formulation of our method. In particular, applying a truncation operation, using only the first 300 generated tokens for score computation, leads to a significant improvement in performance. Secondly, our method achieves better performance after applying the token deviation measure, indicating that focusing on outlier tokens produces a more distinguishable membership signal. Finally, we introduce a α to adjust the contribution of tokens to the score, leading to a significant improvement in the TPR@1%FPR score. By combining these components, we obtain the final formulation of our method, which achieves superior performance in both AUC and TPR@1% FPR scores.

Table 3: **AUC** scores of our method and baselines on the paraphrased S1 dataset, evaluated across different-sized models. **Bold** shows the superior result.

Method	Qwen2.5-7B-Instruct	Qwen2.5-14B-Instruct	Qwen2.5-32B-Instruct
Perplexity (Li, 2023)	0.463	0.468	0.469
Lowercase (Carlini et al., 2021)	0.503	0.493	0.543
Zlib (Carlini et al., 2021)	0.497	0.497	0.496
MIN-K% (Shi et al., 2024)	0.469	0.475	0.473
MIN-K%++ (Zhang et al., 2025b)	0.500	0.494	0.527
Ours	0.615	0.692	0.691

6 DISCUSSION

How does partial availability affect the performance of our method and baselines? To illustrate the scenarios where our method provides utility, we evaluate our method and baselines on the S1 dataset using the Qwen2.5-7B-Instruct model across three distinct settings: (1) using only the question, (2) using the question along with the reasoning trajectories, and (3) using the full sample comprising the question, reasoning trajectories and answer.

We provide the AUC scores of baselines and our method in Appendix C.2. The results show that baseline methods are effective in settings where reasoning trajectories and answers are available, while their performance notably degrades when only the question is available. The finding indicates that partial availability leads to poor performance of baselines in distillation data detection. The results show that our TBD is the only effective method in the Question-Only setting, while all baseline methods fail to detect distillation data. Our method enables effective detection in the realistic and challenging setting, where only the is available, achieving meaningful performance without relying on trajectories or answers.

Is our method effective for question paraphrasing? To examine the performance of our method under reasoning distillation with paraphrased questions, we conduct experiments on the S1 dataset across different models, including Qwen2.5-7B-Instruct, Qwen2.5-14B-Instruct and Qwen2.5-32B-Instruct models. We use GPT-5-mini² to paraphrase the original question, obtaining a rephrased version that remains semantically consistent with the original question. We then evaluate our method on paraphrased questions to simulate a scenario where the original questions used for reasoning distillation are unavailable. The Table 3 reports the AUC scores of baselines and our method. The results show that our method consistently outperforms baselines, indicating its capability to detect distillation data in the question paraphrasing scenario.

7 CONCLUSION

In this work, we first present the problem of distillation data detection and emphasize its unique challenge of partial availability. We propose Token Probability Deviation (TBD), a novel and effective method for detecting distillation data. Our method utilizes generated tokens instead of input sequences to identify data membership. This can be achieved by measuring the deviation of generated tokens' probabilities from a high reference probability. Experimental results show that our method is robust to parameter choice, enabling us to deploy our algorithm without task-specific hyperparameter tuning. In addition, our method can detect distillation data even under a low false-positive rate constraint, showing the practicality of our method in real-world applications. In summary, extensive experiments demonstrate the effectiveness of our method on various datasets across diverse models in distillation data detection. We hope that our study can advance further research on data contamination resulting from reasoning distillation.

Limitations Our work focuses on detecting training data used in reasoning distillation. Our method is limited in the scope of reasoning distillation with supervised fine-tuning, leaving other scenarios to be explored in future work.

²<https://platform.openai.com/docs/models/gpt-5-mini>

540 ETHICS STATEMENT
541542 Our work aims to detect distillation data, a data leakage problem resulting from reasoning distil-
543 lation. The proposed methodology aims to identify data potentially used in reasoning distillation.
544 Regarding data access, the distillation datasets we employed in our work come from prior research
545 and do not involve privacy information. This paper presents work whose goal is to advance research
546 on data contamination resulting from reasoning distillation. There are many potential societal con-
547 sequences of our work, none of which we feel must be specifically highlighted here.
548549 REPRODUCIBILITY STATEMENT
550551 We have made efforts to ensure that the experimental results in this paper are reproducible. We
552 provide an anonymous link to the downloadable source code in the supplementary materials for
553 others to reproduce the results in our experiments. The experimental setup, including training steps,
554 datasets, models and hardware details, is described in detail in this paper. To support reproducibility,
555 we provide detailed instructions on code execution for our experiments. We hope that our efforts
556 can help other researchers reproduce our work and further advance the field.
557558 REFERENCES
559560 Nicholas Carlini, Florian Tramer, Eric Wallace, Matthew Jagielski, Ariel Herbert-Voss, Katherine
561 Lee, Adam Roberts, Tom Brown, Dawn Song, Ulfar Erlingsson, et al. Extracting training data
562 from large language models. In *30th USENIX Security Symposium (USENIX Security 21)*, pp.
563 2633–2650, 2021.564 Nicholas Carlini, Steve Chien, Milad Nasr, Shuang Song, Andreas Terzis, and Florian Tramer. Mem-
565 bership inference attacks from first principles. In *2022 IEEE symposium on security and privacy
(SP)*, pp. 1897–1914. IEEE, 2022.
566568 Kent K Chang, Mackenzie Cramer, Sandeep Soni, and David Bamman. Speak, memory: an archae-
569 ology of books known to chatgpt/gpt-4. *arXiv preprint arXiv:2305.00118*, 2023.
570571 Xiaoshu Chen, Sihang Zhou, Ke Liang, and Xinwang Liu. Distilling reasoning ability from large
572 language models with adaptive thinking. *IEEE Transactions on Neural Networks and Learning
Systems*, 2025.
573574 Hyeong Kyu Choi, Maxim Khanov, Hongxin Wei, and Yixuan Li. How contaminated is your bench-
575 mark? quantifying dataset leakage in large language models with kernel divergence. In *Inter-
576 national Conference on Machine Learning*, 2025.
577578 Gheorghe Comanici, Eric Bieber, Mike Schaeckermann, Ice Pasupat, Noveen Sachdeva, Inderjit
579 Dhillon, Marcel Blstein, Ori Ram, Dan Zhang, Evan Rosen, et al. Gemini 2.5: Pushing the
580 frontier with advanced reasoning, multimodality, long context, and next generation agentic capa-
581 bilities. *arXiv preprint arXiv:2507.06261*, 2025.
582583 Abhimanyu Dubey, Abhinav Jauhri, Abhinav Pandey, Abhishek Kadian, Ahmad Al-Dahle, Aiesha
584 Letman, Akhil Mathur, Alan Schelten, Amy Yang, Angela Fan, et al. The llama 3 herd of models.
585 *arXiv e-prints*, pp. arXiv–2407, 2024.
586587 Wenjie Fu, Huandong Wang, Chen Gao, Guanghua Liu, Yong Li, and Tao Jiang. Membership
588 inference attacks against fine-tuned large language models via self-prompt calibration. *Advances
589 in Neural Information Processing Systems*, 37:134981–135010, 2024.
590591 Michael M Grynbaum and Ryan Mac. The times sues openai and microsoft over ai use of copy-
592 righted work. *The New York Times*, 27, 2023.
593594 Daya Guo, Dejian Yang, Haowei Zhang, Junxiao Song, Ruoyu Zhang, Runxin Xu, Qihao Zhu,
595 Shirong Ma, Peiyi Wang, Xiao Bi, et al. Deepseek-r1: Incentivizing reasoning capability in llms
596 via reinforcement learning. *arXiv preprint arXiv:2501.12948*, 2025.
597

594 Aaron Jaech, Adam Kalai, Adam Lerer, Adam Richardson, Ahmed El-Kishky, Aiden Low, Alec
 595 Helyar, Aleksander Madry, Alex Beutel, Alex Carney, et al. Openai o1 system card. *arXiv*
 596 *preprint arXiv:2412.16720*, 2024.

597

598 Albert Q. Jiang, Alexandre Sablayrolles, Arthur Mensch, Chris Bamford, Devendra Singh Chap-
 599 lot, Diego de las Casas, Florian Bressand, Gianna Lengyel, Guillaume Lample, Lucile Saulnier,
 600 Lélio Renard Lavaud, Marie-Anne Lachaux, Pierre Stock, Teven Le Scao, Thibaut Lavril,
 601 Thomas Wang, Timothée Lacroix, and William El Sayed. Mistral 7b, 2023. URL <https://arxiv.org/abs/2310.06825>.

602

603 Aviral Kumar, Vincent Zhuang, Rishabh Agarwal, Yi Su, John D Co-Reyes, Avi Singh, Kate Baumli,
 604 Shariq Iqbal, Colton Bishop, Rebecca Roelofs, et al. Training language models to self-correct via
 605 reinforcement learning. *arXiv preprint arXiv:2409.12917*, 2024.

606

607 Bespoke Labs. Bespoke-stratos: The unreasonable effectiveness of reasoning dis-
 608 tillation. <https://www.bespokelabs.ai/blog/bespoke-stratos-the-unreasonable-effectiveness-of->
 609 reasoning-distillation, 2025. Accessed: 2025-01-22.

610

611 Xinhe Li, Jiajun Liu, and Peng Wang. Can large models teach student models to solve mathematical
 612 problems like human beings? a reasoning distillation method via multi-lora interaction, 2025.
 613 URL <https://arxiv.org/abs/2508.13037>.

614

615 Yucheng Li. Estimating contamination via perplexity: quantifying memorisation in language model
 616 evaluation. *arXiv preprint arXiv:2309.10677*, 2023.

617

618 Wanlong Liu, Junxiao Xu, Fei Yu, Yukang Lin, Ke Ji, Wenyu Chen, Yan Xu, Yasheng Wang, Lifeng
 619 Shang, and Benyou Wang. Qfft, question-free fine-tuning for adaptive reasoning. *arXiv preprint*
 620 *arXiv:2506.12860*, 2025.

621

622 Ziyang Ma, Qingyue Yuan, Linhai Zhang, and Deyu Zhou. Slow tuning and low-entropy masking
 623 for safe chain-of-thought distillation. *arXiv preprint arXiv:2508.09666*, 2025.

624

625 Justus Mattern, Fatemehsadat Mireshghallah, Zhijing Jin, Bernhard Schoelkopf, Mrinmaya Sachan,
 626 and Taylor Berg-Kirkpatrick. Membership inference attacks against language models via neigh-
 627 bourhood comparison. In *Findings of the Association for Computational Linguistics: ACL 2023*,
 628 pp. 11330–11343, 2023.

629

630 Fatemehsadat Mireshghallah, Kartik Goyal, Archit Uniyal, Taylor Berg-Kirkpatrick, and Reza
 631 Shokri. Quantifying privacy risks of masked language models using membership inference at-
 632 tacks. *arXiv preprint arXiv:2203.03929*, 2022.

633

634 Maximilian Mozes, Xuanli He, Bennett Kleinberg, and Lewis D Griffin. Use of llms for illicit
 635 purposes: Threats, prevention measures, and vulnerabilities. *arXiv preprint arXiv:2308.12833*,
 636 2023.

637

638 Niklas Muennighoff, Zitong Yang, Weijia Shi, Xiang Lisa Li, Li Fei-Fei, Hannaneh Hajishirzi, Luke
 639 Zettlemoyer, Percy Liang, Emmanuel Candes, and Tatsunori Hashimoto. s1: Simple test-
 640 time scaling. In *Workshop on Reasoning and Planning for Large Language Models*, 2025a. URL
 641 <https://openreview.net/forum?id=LdH0vrgAHm>.

642

643 Niklas Muennighoff, Zitong Yang, Weijia Shi, Xiang Lisa Li, Li Fei-Fei, Hannaneh Hajishirzi, Luke
 644 Zettlemoyer, Percy Liang, Emmanuel Candès, and Tatsunori Hashimoto. s1: Simple test-time
 645 scaling. *arXiv preprint arXiv:2501.19393*, 2025b.

646

647 Yonatan Oren, Nicole Meister, Niladri S Chatterji, Faisal Ladhak, and Tatsunori Hashimoto. Proving
 648 test set contamination in black-box language models. In *ICLR*, 2024a.

649

650 Yonatan Oren, Nicole Meister, Niladri S Chatterji, Faisal Ladhak, and Tatsunori Hashimoto. Proving
 651 test set contamination in black-box language models. In *The Twelfth International Conference on*
 652 *Learning Representations*, 2024b.

648 Qwen, :, An Yang, Baosong Yang, Beichen Zhang, Binyuan Hui, Bo Zheng, Bowen Yu, Chengyuan
 649 Li, Dayiheng Liu, Fei Huang, Haoran Wei, Huan Lin, Jian Yang, Jianhong Tu, Jianwei Zhang,
 650 Jianxin Yang, Jiaxi Yang, Jingren Zhou, Junyang Lin, Kai Dang, Keming Lu, Keqin Bao, Kexin
 651 Yang, Le Yu, Mei Li, Mingfeng Xue, Pei Zhang, Qin Zhu, Rui Men, Runji Lin, Tianhao Li,
 652 Tianyi Tang, Tingyu Xia, Xingzhang Ren, Xuancheng Ren, Yang Fan, Yang Su, Yichang Zhang,
 653 Yu Wan, Yuqiong Liu, Zeyu Cui, Zhenru Zhang, and Zihan Qiu. Qwen2.5 technical report, 2025.
 654 URL <https://arxiv.org/abs/2412.15115>.

655 Negin Raoof, Litu Rout, Giannis Daras, Sujay Sanghavi, Constantine Caramanis, Sanjay Shakkottai,
 656 and Alex Dimakis. Infilling score: A pretraining data detection algorithm for large language
 657 models. In *The Thirteenth International Conference on Learning Representations*, 2025. URL
 658 <https://openreview.net/forum?id=9QPH1YQCMn>.

659 Weijia Shi, Anirudh Ajith, Mengzhou Xia, Yangsibo Huang, Daogao Liu, Terra Blevins, Danqi
 660 Chen, and Luke Zettlemoyer. Detecting pretraining data from large language models. In *The*
 661 *Twelfth International Conference on Learning Representations*, 2024.

662 Reza Shokri, Marco Stronati, Congzheng Song, and Vitaly Shmatikov. Membership inference at-
 663 tacks against machine learning models. In *2017 IEEE Symposium on Security and Privacy (SP)*,
 664 pp. 3–18. IEEE Computer Society, 2017.

665 Gemma Team, Thomas Mesnard, Cassidy Hardin, Robert Dadashi, Surya Bhupatiraju, Shreya
 666 Pathak, Laurent Sifre, Morgane Rivière, Mihir Sanjay Kale, Juliette Love, et al. Gemma: Open
 667 models based on gemini research and technology. *arXiv preprint arXiv:2403.08295*, 2024.

668 NovaSky Team. Sky-t1: Train your own o1 preview model within 450. <https://novasky-ai.github.io/posts/sky-t1>, 2025. Accessed: 2025-01-09.

669 Yijun Tian, Yikun Han, Xiusi Chen, Wei Wang, and Nitesh V Chawla. Beyond answers: Trans-
 670 ferring reasoning capabilities to smaller llms using multi-teacher knowledge distillation. In *Pro-
 671 ceedings of the Eighteenth ACM International Conference on Web Search and Data Mining*, pp.
 672 251–260, 2025.

673 Ziyu Wan, Xidong Feng, Muning Wen, Stephen Marcus Mcalleer, Ying Wen, Weinan Zhang, and
 674 Jun Wang. Alphazero-like tree-search can guide large language model decoding and training. In
 675 *International Conference on Machine Learning*, pp. 49890–49920. PMLR, 2024.

676 Jason Wei, Xuezhi Wang, Dale Schuurmans, Maarten Bosma, Fei Xia, Ed Chi, Quoc V Le, Denny
 677 Zhou, et al. Chain-of-thought prompting elicits reasoning in large language models. *Advances in*
 678 *neural information processing systems*, 35:24824–24837, 2022.

679 Juncheng Wu, Wenlong Deng, Xingxuan Li, Sheng Liu, Taomian Mi, Yifan Peng, Ziyang Xu,
 680 Yi Liu, Hyunjin Cho, Chang-In Choi, et al. Medreason: Eliciting factual medical reasoning
 681 steps in llms via knowledge graphs. *arXiv preprint arXiv:2504.00993*, 2025a.

682 Xiaojun Wu, Xiaoguang Jiang, Huiyang Li, Jucai Zhai, Dengfeng Liu, Qiaobo Hao, Huang Liu,
 683 Zhiguo Yang, Ji Xie, Ninglun Gu, et al. Beyond scaling law: A data-efficient distillation frame-
 684 work for reasoning. *arXiv preprint arXiv:2508.09883*, 2025b.

685 xAI. Grok 3 beta — the age of reasoning agents, 2025. URL <https://x.ai/news/grok-3>.

686 Huajian Xin, ZZ Ren, Junxiao Song, Zhihong Shao, Wanja Zhao, Haocheng Wang, Bo Liu, Liyue
 687 Zhang, Xuan Lu, Qiushi Du, et al. Deepseek-prover-v1. 5: Harnessing proof assistant feedback
 688 for reinforcement learning and monte-carlo tree search. *arXiv preprint arXiv:2408.08152*, 2024.

689 Cheng Xu, Shuhao Guan, Derek Greene, M Kechadi, et al. Benchmark data contamination of large
 690 language models: A survey. *arXiv preprint arXiv:2406.04244*, 2024a.

691 Ruijie Xu, Zengzhi Wang, Run-Ze Fan, and Pengfei Liu. Benchmarking benchmark leakage in large
 692 language models. *arXiv e-prints*, pp. arXiv–2404, 2024b.

693 An Yang, Anfeng Li, Baosong Yang, Beichen Zhang, Binyuan Hui, Bo Zheng, Bowen Yu,
 694 Chang Gao, Chengen Huang, Chenxu Lv, et al. Qwen3 technical report. *arXiv preprint*
 695 *arXiv:2505.09388*, 2025.

702 Yixin Ye, Zhen Huang, Yang Xiao, Ethan Chern, Shijie Xia, and Pengfei Liu. Limo: Less is more
703 for reasoning. *arXiv preprint arXiv:2502.03387*, 2025.
704

705 Hengxiang Zhang, Songxin Zhang, Bingyi Jing, and Hongxin Wei. Fine-tuning can help de-
706 tect pretraining data from large language models. In *The Thirteenth International Confer-
707 ence on Learning Representations*, 2025a. URL <https://openreview.net/forum?id=X8dzvdkQwO>
708

709 Jingyang Zhang, Jingwei Sun, Eric Yeats, Yang Ouyang, Martin Kuo, Jianyi Zhang, Hao Frank
710 Yang, and Hai Li. Min-k%++: Improved baseline for pre-training data detection from large lan-
711 guage models. In *The Thirteenth International Conference on Learning Representations*, 2025b.
712 URL <https://openreview.net/forum?id=ZGkfoufDaU>.
713

714 Xianwei Zhuang, Zhihong Zhu, Zhichang Wang, Xuxin Cheng, and Yuexian Zou. Unicott: A unified
715 framework for structural chain-of-thought distillation. In *The Thirteenth International Conference
on Learning Representations*, 2025.
716
717
718
719
720
721
722
723
724
725
726
727
728
729
730
731
732
733
734
735
736
737
738
739
740
741
742
743
744
745
746
747
748
749
750
751
752
753
754
755

756 757 758 759 Appendix 760 761

762 Table of Contents

763	A Related Works	15
764		
765	B Experimental Details	16
766	B.1 Details of Datasets and Models	16
767	B.2 Training Details	16
768	B.3 Implementation Examples	17
769		
770	C Additional Results	20
771	C.1 Token-wise Probability Distribution	20
772	C.2 Experimental Results	21
773		
774	D Use of Large Language Models	21
775		
776		

777 A RELATED WORKS

778 In this paper, we propose a problem about distillation data detection, which is related to an amount of
779 literature on reasoning distillation and detecting training data from Large Language Models (LLMs).
780 We discuss related works in two directions relevant to our study.

781 **Distilling reasoning capability from LRM**s. Large Reasoning Models (LRMs) exhibit remarkable
782 performance in solving complex tasks, achieving this by training the model to produce a long
783 chain of thought reasoning process before responding with the final answer (Jaech et al., 2024; Yang
784 et al., 2025; Comanici et al., 2025). However, developing reasoning models, which achieve reasoning
785 capacity compared to large reasoning models, remains a significant challenge for the research
786 community (Kumar et al., 2024; Xin et al., 2024; Wan et al., 2024). Recently, a growing literature
787 has focused on reasoning distillation, which improves the reasoning capabilities of models with
788 lower computational cost (Guo et al., 2025; Yang et al., 2025; Wu et al., 2025b; Ma et al., 2025).
789 In practice, distillation methods often employ supervised fine-tuning to enable a model to mimic
790 reasoning trajectories generated by large reasoning models (Guo et al., 2025; Muennighoff et al.,
791 2025b; Ye et al., 2025; Liu et al., 2025). For instance, S1 (Muennighoff et al., 2025b) and LIMO (Ye
792 et al., 2025) enhance the reasoning capacity of small language models by fine-tuning models on
793 well-crafted distillation datasets. However, training models on distillation datasets that overlap with
794 benchmark data can inflate the performance of distilled models. Thus, our work aims to develop
795 detection methods for identifying distillation data potentially used in reasoning distillation.

796 **Detecting training data from LLM**s. Training data detection on LLMs has been studied in previous
797 works, encompassing fine-tuning data detection and pretraining data detection (Mattern et al.,
798 2023; Fu et al., 2024; Zhang et al., 2025b; Shi et al., 2024; Raoof et al., 2025). Training data may
799 pose risks such as privacy leakage, where training data containing personal information may lead
800 to privacy leakage (Grynbaum & Mac, 2023; Mozes et al., 2023). Furthermore, the training dataset
801 may inadvertently include data from benchmarks, which compromises the reliability of benchmark
802 evaluations (Oren et al., 2024b; Choi et al., 2025; Xu et al., 2024b). Fine-tuning data detection for
803 LLMs aim to determine the training data used for fine-tuning (Mattern et al., 2023; Mireshghallah
804 et al., 2022). The repeated exposure of the fine-tuning data across multiple training epochs increases
805 their vulnerability to privacy attacks. Pretraining data detection aims to determine whether a piece of
806 text is included in the pretraining dataset (Zhang et al., 2025a). The task is particularly challenging
807 due to the massive scale of the pretraining corpus and the fact that pretraining usually runs for only
808 one epoch (Shi et al., 2024). Previous studies often design scoring functions that compute a score
809 for each input sequence to detect training data from LLMs (Zhang et al., 2025b). Our work proposes

810 a problem of distillation data detection and a novel and effective method, which leverages generated
 811 tokens instead of the input sequence to detect distillation data.
 812

814 B EXPERIMENTAL DETAILS

816 B.1 DETAILS OF DATASETS AND MODELS

820 **Datasets and Models.** To obtain diverse distilled reasoning models, we fine-tune different mod-
 821 els on three well-crafted distillation datasets, including S1, S1.1 (Muennighoff et al., 2025b) and
 822 LIMO (Ye et al., 2025). Use questions as prompts, developers often generate reasoning trajectories
 823 along with the final answer from advanced large reasoning models to construct distillation datasets.
 824 The S1 and S1.1 datasets contain 1,000 examples, whose reasoning trajectories are produced from
 825 Gemini (Comanici et al., 2025) and DeepSeek-R1 (Guo et al., 2025), respectively. LIMO is a high-
 826 quality distillation dataset containing only 817 examples, where each example contains a question
 827 together with the reasoning trajectory and final answer. [We provide details of the distillation datasets](#)
 828 [in Table 4](#). [As described in Appendix B.3, we present the illustration of a sample comprising a](#)
 829 [question, corresponding reasoning trajectories, and the final answer.](#) In our experiments, following
 830 previous work (Muennighoff et al., 2025b; Ye et al., 2025; Liu et al., 2025), we conduct experiments
 831 on different base models, including the Qwen2.5-7B-Instruct, Qwen2.5-14B-Instruct and Qwen2.5-
 832 32B-Instruct models (Qwen et al., 2025). Specifically, we fine-tune these models on the distillation
 833 dataset, enabling models to imitate reasoning trajectories generated by teacher models.
 834

835 Table 4: Detailed statistics of distillation datasets.

836 Datasets	837 Samples	838 Avg. Tokens per sample	839 Domain	840 Source model	841 Link
838 LIMO (Ye et al., 2025)	817	7126	839 Math	840 QwQ-32B, etc.	841 Dataset
839 S1 (Muennighoff et al., 2025b)	1000	5058	840 Math, Science	841 Gemini	842 Dataset
840 S1.1 (Muennighoff et al., 2025a)	1000	10038	841 Math, Science	842 DeepSeek-R1	843 Dataset

844 B.2 TRAINING DETAILS

846 In our experiments, we fine-tune different base models on distillation datasets to obtain distilled
 847 reasoning models. In particular, we perform full-parameter fine-tuning on 8 A100 GPUs using
 848 DeepSpeed ZeRO-3 optimization, with a sequence length limit of 16,384 tokens. In Table 5, we
 849 report detailed training parameters employed in the supervised fine-tuning process.
 850

851 Table 5: Hyperparameters used for supervised fine-tuning.

853 Hyperparameter	854 S1	855 S1.1	856 LIMO
854 sequence length	855 16384	856 16384	857 16384
855 batch size	856 8	857 8	858 8
856 learning rate	857 1e-5	858 1e-5	859 1e-5
857 epochs	858 5	859 5	860 5
858 scheduler	859 cosine	860 cosine	861 cosine
859 weight decay	860 1e-4	861 1e-4	862 1e-4
860 zero optimization	861 ZeRO-3	862 ZeRO-3	863 ZeRO-3
861 training precision	862 bf16	863 bf16	bf16

864 B.3 IMPLEMENTATION EXAMPLES
865866 We provide examples of distillation data and question prompts in Example B.1 and Example B.2. A
867 datapoint from the S1 distillation dataset (Muennighoff et al., 2025b) is presented in Example B.1,
868 comprising a question, corresponding reasoning trajectories, and final answer. In Example B.2, we
869 present three question prompts using the system template.
870871 **Example B.1: Illustrative case of distillation data**
872873 **Question:**
874 Given a rational number, write it as a fraction in lowest terms and calculate the product of the
875 resulting numerator and denominator. For how many rational numbers between 0 and 1 will 20!
876 be the resulting product?
877878 **Thinking Trajectories:**
879 The problem asks for the number of rational numbers between 0 and 1 such that when the
880 rational number is written as a fraction in lowest terms, the product of the numerator and the
881 denominator is 20!.
882 Let the rational number be r , where $0 < r < 1$. We can write r as a fraction $\frac{a}{b}$, where a and b
883 are positive integers, and $\gcd(a, b) = 1$. Since $0 < r < 1$, we have $0 < \frac{a}{b} < 1$, which implies
884 $0 < a < b$. The product of the numerator and the denominator of the fraction in lowest terms is
885 $a \times b$. We are given that $a \times b = 20!$. We need to find the number of pairs (a, b) such that:
886 1. a and b are positive integers.
887 2. $\gcd(a, b) = 1$.
888 3. $a < b$.
889 4. $a \times b = 20!$.
890 Let $N = 20!$. We have $a \times b = N$. Since $\gcd(a, b) = 1$, the prime factors of N are distributed
891 between a and b such that no prime factor is shared by both. Consider the prime factorization of
892 $N = 20!$. Let $N = p_1^{e_1} p_2^{e_2} \cdots p_k^{e_k}$, where p_i are distinct prime numbers and $e_i \geq 1$.
893 Since $a \times b = N$ and $\gcd(a, b) = 1$, each prime power $p_i^{e_i}$ must be entirely a factor of a or
894 entirely a factor of b . For each prime power $p_i^{e_i}$, there are two choices: either $p_i^{e_i}$ is a factor of a ,
895 or $p_i^{e_i}$ is a factor of b . Since there are k distinct prime factors, there are 2^k ways to distribute the
896 prime power factors between a and b . Each way corresponds to a unique pair (a, b) such that
897 $a \times b = N$ and $\gcd(a, b) = 1$. Let the number of distinct prime factors of $N = 20!$ be $\omega(20!)$.
898 Then the number of pairs (a, b) such that $a \times b = 20!$ and $\gcd(a, b) = 1$ is $2^{\omega(20!)}$. Now, we
899 need to consider the condition $a < b$. Since $a \times b = N$, if $a \neq b$, then either $a < b$ or $b < a$. If
900 $a = b$, then $a^2 = N$, which means N is a perfect square. $20!$ is not a perfect square because
901 the exponent of some prime factors in its prime factorization is odd (e.g., the exponent of the
902 largest prime less than or equal to 20, which is 19). The pairs (a, b) such that $a \times b = N$ and
903 $\gcd(a, b) = 1$ can be grouped into pairs of the form (a, b) and (b, a) , where $a \neq b$. The number
904 of such pairs is $2^{\omega(N)}$. Each pair contributes to either $a < b$ or $b < a$. Since $a \neq b$, exactly half
905 of these pairs will satisfy $a < b$.
906 The number of pairs (a, b) such that $a \times b = N$, $\gcd(a, b) = 1$, and $a < b$ is
907 $\frac{1}{2} \times 2^{\omega(N)} = 2^{\omega(N)-1}$. We need to find the number of distinct prime factors of $20!$.
908 The prime numbers less than or equal to 20 are 2, 3, 5, 7, 11, 13, 17, 19. There are 8 distinct
909 prime factors of $20!$. So, $\omega(20!) = 8$. The number of pairs (a, b) satisfying the conditions is
910 $2^{8-1} = 2^7 = 128$. Each such pair (a, b) corresponds to a unique rational number $\frac{a}{b}$ between 0
911 and 1 in lowest terms, where $a \times b = 20!$. The number of rational numbers between 0 and 1
912 for which the product of the numerator and denominator of the fraction in lowest terms is $20!$ is
913 128. Let's verify the reasoning. Consider a simpler example: Product is 12. Prime factorization
914 of 12 is $2^2 \times 3^1$. Distinct prime factors are 2 and 3. $\omega(12) = 2$. Pairs (a, b) such that $a \times b = 12$
915 and $\gcd(a, b) = 1$: Factors of 12 are 1, 2, 3, 4, 6, 12. Possible pairs (a, b) with $a \times b = 12$: (1,
916 12), (2, 6), (3, 4). Check $\gcd(a, b) = 1$: $\gcd(1, 12) = 1$ $\gcd(2, 6) = 2 \neq 1$ $\gcd(3, 4) = 1$
917 The pairs (a, b) such that $a \times b = 12$ and $\gcd(a, b) = 1$ are formed by distributing the prime
918 factors 2^2 and 3^1 . a can have factors from $\{1, 2^2, 3^1, 2^2 \times 3^1\}$ and b will have the remaining

918
919
920

factors. Case 1: $a = 1, b = 12$. $\gcd(1, 12) = 1$. Case 2: $a = 4, b = 3$. $\gcd(4, 3) = 1$. Case 3: $a = 3, b = 4$. $\gcd(3, 4) = 1$. Case 4: $a = 12, b = 1$. $\gcd(12, 1) = 1$.

921
922
923
924
925
926
927
928
929
930
931
932
933
934
935

Something is wrong here. Let's use the prime factorization directly. $12 = 2^2 \times 3^1$. Prime factors are 2 and 3. Possible distributions of prime powers:- a has $2^0, 3^0$, b has $2^2, 3^1 \implies a = 1, b = 12$. $\gcd(1, 12) = 1$. a has $2^2, 3^0$, b has $2^0, 3^1 \implies a = 4, b = 3$. $\gcd(4, 3) = 1$. a has $2^0, 3^1$, b has $2^2, 3^0 \implies a = 3, b = 4$. $\gcd(3, 4) = 1$. a has $2^2, 3^1$, b has $2^0, 3^0 \implies a = 12, b = 1$. $\gcd(12, 1) = 1$. The pairs (a, b) such that $a \times b = 12$ and $\gcd(a, b) = 1$ are $(1, 12)$ and $(4, 3)$ and $(3, 4)$ and $(12, 1)$. Number of such pairs is $2^{\omega(12)} = 2^2 = 4$. Now, consider the condition $a < b$. Pairs where $a < b$: $(1, 12)$ and $(3, 4)$. Number of such pairs is $\frac{1}{2} \times 4 = 2$. The rational numbers are $\frac{1}{12}$ and $\frac{3}{4}$. Product of numerator and denominator: $1 \times 12 = 12, 3 \times 4 = 12$. Fractions are in lowest terms. Rational numbers are between 0 and 1. The number of distinct prime factors of $20!$ needs to be correctly calculated. Prime numbers ≤ 20 : 2, 3, 5, 7, 11, 13, 17, 19. There are 8 distinct prime factors. Let $N = 20!$. We are looking for rational numbers $\frac{a}{b}$ such that $\gcd(a, b) = 1$, $0 < a < b$, and $a \times b = N$. The number of pairs (a, b) such that $a \times b = N$ and $\gcd(a, b) = 1$ is $2^{\omega(N)}$. Each pair corresponds to a factorization of N into two coprime factors. Let $N = p_1^{e_1} p_2^{e_2} \cdots p_k^{e_k} \cdot a = p_1^{\alpha_1} p_2^{\alpha_2} \cdots p_k^{\alpha_k} b = p_1^{\beta_1} p_2^{\beta_2} \cdots p_k^{\beta_k}$

936
937
938
939
940
941
942
943
944
945
946
947
948
949
950
951

Since $\gcd(a, b) = 1$, for each i , either $\alpha_i = e_i, \beta_i = 0$ or $\alpha_i = 0, \beta_i = e_i$. This gives 2^k choices for the pair (a, b) . We need $a < b$. Consider the case $a = b$. This happens only if all prime exponents e_i are even, which is not the case for $20!$. So, for every pair (a, b) with $a \times b = N$ and $\gcd(a, b) = 1$, we have $a \neq b$. The pairs can be grouped into (a, b) and (b, a) , where $a \neq b$. The number of such pairs is $2^{\omega(N)}$. The number of pairs with $a < b$ is $\frac{1}{2} \times 2^{\omega(N)} = 2^{\omega(N)-1}$. For $N = 20!$, $\omega(N) = 8$. The number of pairs (a, b) is $2^{8-1} = 2^7 = 128$. Each pair (a, b) corresponds to a unique rational number $\frac{a}{b}$ between 0 and 1 in lowest terms, such that $a \times b = 20!$. Double-check the problem statement and constraints. Rational numbers between 0 and 1. Resulting product of numerator and denominator is $20!$. Consider a rational number r between 0 and 1. When written as a fraction in lowest terms, let it be $\frac{a}{b}$, where $\gcd(a, b) = 1$ and $0 < a < b$. We are given $a \times b = 20!$. We need to find the number of such fractions $\frac{a}{b}$. This is equivalent to finding the number of pairs (a, b) satisfying the conditions. The number of distinct prime factors of $20!$ is the number of primes less than or equal to 20, which is 8. The primes are 2, 3, 5, 7, 11, 13, 17, 19. Let the prime factorization of $20!$ be $p_1^{e_1} p_2^{e_2} \cdots p_8^{e_8} \cdot a \times b = p_1^{e_1} p_2^{e_2} \cdots p_8^{e_8} \cdot b$. Since $\gcd(a, b) = 1$, for each prime factor p_i , either $p_i^{e_i}$ is a factor of a or $p_i^{e_i}$ is a factor of b .

952
953
954
955
956
957
958
959
960
961
962
963
964
965

Consider the divisors of $20!$ that are coprime to their cofactors in the division. If d is a divisor of N , then $N = d \times \frac{N}{d}$. We need $\gcd(d, \frac{N}{d}) = 1$. This means that the prime factors of d and $\frac{N}{d}$ are disjoint. Equivalently, for each prime factor p_i of N , either $p_i^{e_i}$ divides d or $p_i^{e_i}$ divides $\frac{N}{d}$. Let a be a divisor of $20!$ such that $\gcd(a, \frac{20!}{a}) = 1$. Then $b = \frac{20!}{a}$. The number of such divisors a is $2^{\omega(20!)}$. These divisors correspond to the possible values of the numerator a in the pairs (a, b) where $a \times b = 20!$ and $\gcd(a, b) = 1$. The pairs are formed by choosing, for each prime power $p_i^{e_i}$, whether it belongs to a or b . Example: $12 = 2^2 \times 3^1$. Prime powers are 2^2 and 3^1 . Choices for factors of a : $\{1, 4\}$, choices for factors of b : $\{1, 3\}$. Possible values of a : $1 \times 1 = 1, 1 \times 3 = 3, 4 \times 1 = 4, 4 \times 3 = 12$. If $a = 1, b = 12$. If $a = 3, b = 4$. If $a = 4, b = 3$. If $a = 12, b = 1$. The pairs (a, b) such that $a \times b = N$ and $\gcd(a, b) = 1$ are formed by partitioning the set of prime power factors into two sets, one for a and one for b . Let the prime power factors be P_1, P_2, \dots, P_k , where $P_i = p_i^{e_i} \cdot a$ is a product of some of these P_i , and b is the product of the remaining ones. For each P_i , it either goes to a or b . 2^k possibilities.

966
967
968
969
970
971

We need $a < b$. Since $a \times b = N$, and $a \neq b$ (as N is not a perfect square), either $a < b$ or $b < a$. The number of pairs with $a < b$ is equal to the number of pairs with $b < a$. Total number of pairs is 2^k . Number of pairs with $a < b$ is $\frac{2^k}{2} = 2^{k-1}$. Here $k = \omega(20!) = 8$. Number of pairs (a, b) with $a < b$, $\gcd(a, b) = 1$, $a \times b = 20!$ is $2^{8-1} = 2^7 = 128$. Each such pair (a, b) corresponds to a unique rational number $\frac{a}{b}$ between 0 and 1 in lowest terms, with the product of numerator

972 and denominator equal to $20!$. Example revisited: Product is 12. Prime factors 2, 3. $\omega(12) = 2$.
 973 Pairs (a, b) with $a \times b = 12$, $\gcd(a, b) = 1$: $a = 1, b = 12$; $a = 3, b = 4$; $a = 4, b = 3$; $a = 12, b = 1$
 974 Pairs with $a < b$: $(1, 12)$, $(3, 4)$. Number $= 2^{2-1} = 2^1 = 2$. Rational numbers: $\frac{1}{12}, \frac{3}{4}$. Consider
 975 the edge cases or potential pitfalls. The condition between 0 and 1 ensures $a < b$. The condition
 976 fraction in lowest terms ensures $\gcd(a, b) = 1$. The problem boils down to finding the number
 977 of ways to factor $20!$ into two coprime factors a and b such that $a < b$. Final confirmation of
 978 the number of distinct prime factors of $20!$: Primes ≤ 20 : 2, 3, 5, 7, 11, 13, 17, 19. There are 8
 979 distinct prime factors. The number of rational numbers is the number of pairs (a, b) satisfying
 980 the conditions, which is $2^{\omega(20!)-1} = 2^{8-1} = 2^7 = 128$. The question asks for how many
 981 rational numbers; so the answer should be the number of such fractions. Each valid pair (a, b)
 982 corresponds to one rational number. If the product was a perfect square, say $36 \cdot 36 = 2^2 \times 3^2$.
 983 $\omega(36) = 2$. Pairs (a, b) with $a \times b = 36$, $\gcd(a, b) = 1$: $a=1, b=36$; $a=4, b=9$; $a=9, b=4$
 984 $a=36, b=1$. Here $a \neq b$. If the product was p^e , where p is prime. Pairs $(1, p^e)$ and $(p^e, 1)$. If
 985 $e > 0$, $1 < p^e$. Rational number $\frac{1}{p^e}$. If the product was pq , where p, q are distinct primes. Pairs
 986 $(1, pq)$, (p, q) , (q, p) , $(pq, 1)$. If $p < q$, then $p < q$, $1 < pq$. Pairs with $a < b$: $(1, pq)$, (p, q) .
 987 Number $= 2^{2-1} = 2$. Rational numbers: $\frac{1}{pq}, \frac{p}{q}$. The reasoning seems consistent. The number of
 988 rational numbers is indeed $2^{\omega(20!)-1}$.
 989

990 **Answer:**

991 Solution: Let the rational number between 0 and 1 be r . When written as a fraction in lowest
 992 terms, let it be $\frac{a}{b}$, where a and b are positive integers, $\gcd(a, b) = 1$, and $0 < a < b$. We are
 993 given that the product of the numerator and denominator is $20!$, so $a \times b = 20!$. We need to find
 994 the number of pairs (a, b) such that $a \times b = 20!$, $\gcd(a, b) = 1$, and $a < b$. Let $N = 20!$. The
 995 prime factorization of N is $p_1^{e_1} p_2^{e_2} \cdots p_k^{e_k}$, where p_i are distinct prime numbers. The number of
 996 distinct prime factors of $20!$ is the number of primes less than or equal to 20. These primes are
 997 2, 3, 5, 7, 11, 13, 17, 19. Thus, there are 8 distinct prime factors, so $k = 8$.
 998

999 Since $a \times b = N$ and $\gcd(a, b) = 1$, each prime power factor $p_i^{e_i}$ of N must be entirely a
 1000 factor of a or entirely a factor of b . The number of ways to distribute the prime power factors
 1001 between a and b is 2^k , where k is the number of distinct prime factors of N . Each distribution
 1002 corresponds to a unique pair (a, b) such that $a \times b = N$ and $\gcd(a, b) = 1$. The number of such
 1003 pairs is $2^{\omega(N)}$, where $\omega(N)$ is the number of distinct prime factors of N .
 1004

1005 Since $20!$ is not a perfect square, for every pair (a, b) such that $a \times b = 20!$ and $\gcd(a, b) = 1$,
 1006 we have $a \neq b$. The pairs can be grouped into (a, b) and (b, a) , where $a \neq b$. The number of
 1007 pairs with $a < b$ is equal to the number of pairs with $b < a$. The total number of pairs is $2^{\omega(20!)}$.
 1008 The number of pairs with $a < b$ is $\frac{1}{2} \times 2^{\omega(20!)} = 2^{\omega(20!)-1}$.
 1009

1010 The number of distinct prime factors of $20!$ is $\omega(20!) = 8$. The number of pairs (a, b) such that
 1011 $a \times b = 20!$, $\gcd(a, b) = 1$, and $a < b$ is $2^{8-1} = 2^7 = 128$. Each such pair (a, b) corresponds to
 1012 a unique rational number $\frac{a}{b}$ between 0 and 1 in lowest terms, with the product of the numerator
 1013 and denominator equal to $20!$.
 1014

1015 Final Answer: The final answer is 128
 1016

1017 **Example B.2: Illustrative case of prompts**

1018 **Prompt1:**

1019 <|im_start|>system
 1020 You are Qwen, created by Alibaba Cloud. You are a helpful assistant. <|im_end|>
 1021 <|im_start|>user
 1022 Given a rational number, write it as a fraction in lowest terms and calculate
 1023 the product of the resulting numerator and denominator. For how many rational
 1024 numbers between 0 and 1 will $\$20_{-}{}^{\{1\}}\$$ be the resulting product?<|im_end|>
 1025 <|im_start|>assistant

```

1026
1027 Prompt2:
1028 <|im_start|>system
1029 You are Qwen, created by Alibaba Cloud. You are a helpful assistant.<|im_end|>
1030 <|im_start|>user
1031 Joanie takes a  $\$6,000$  loan to pay for her car. The annual interest rate on
1032 the loan is  $12\%$ . She makes no payments for 4 years, but has to pay back all
1033 the money she owes at the end of 4 years. How much more money will she owe if
1034 the interest compounds quarterly than if the interest compounds annually?
1035 Express your answer as a dollar value to the nearest cent.<|im_end|>
1036 <|im_start|>assistant
1037
1038 Prompt3:
1039 You are Qwen, created by Alibaba Cloud. You are a helpful assistant.<|im_end|>
1040 <|im_start|>user
1041 Gary purchased a large beverage, but only drank  $m/n$  of it, where  $m$  and  $n$ 
1042 are relatively prime positive integers. If he had purchased half as much and
1043 drunk twice as much, he would have wasted only  $2/9$  as much beverage. Find  $m+n$ 
1044 .<|im_end|>
1045 <|im_start|>assistant

```

C ADDITIONAL RESULTS

C.1 TOKEN-WISE PROBABILITY DISTRIBUTION

To compare the probability distribution differences in generated tokens, we analyze the first 300 generated tokens and the generated tokens at positions 700–1000 for both members and non-members. Figure 6 shows the token-wise probability distributions from the distilled reasoning model across 20 member and 20 non-member samples. We find the generated tokens at positions 700–1000 exhibit only minor probability distribution differences between members and non-members (Right). This pattern is significantly different from the generation behavior in the first 300 generated tokens (Left), where members tend to produce high-probability tokens, whereas non-members induce more low-probability tokens. The disparity indicates that earlier generated tokens are likely to exhibit distinct membership signals for members and non-members.

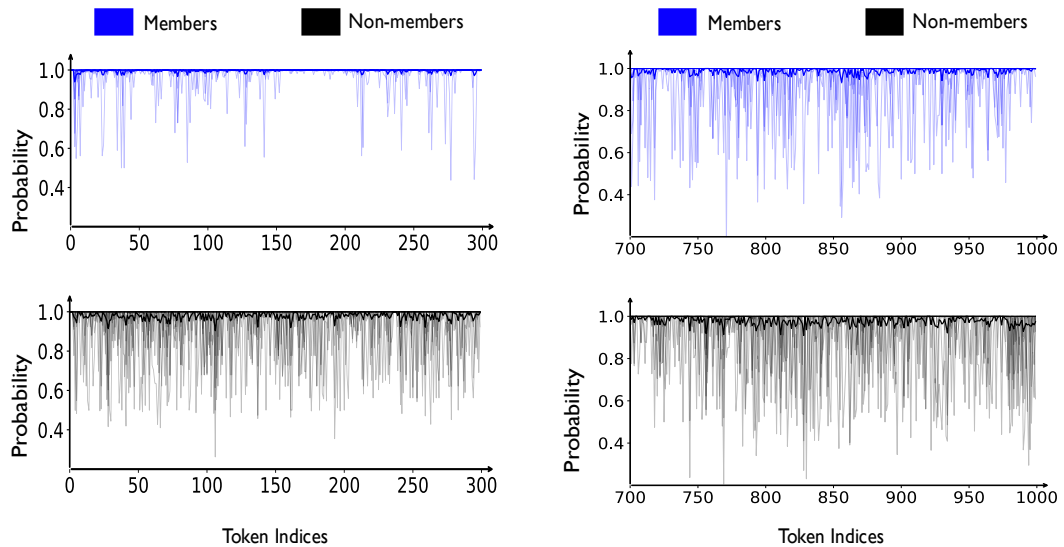


Figure 6: Comparison of token-level generation behaviour of distilled models for 20 member and 20 non-member questions under greedy decoding. **(Left) Token-wise probability distributions of the first 300 generated tokens:** we contrast the distribution of token-wise probability between members and non-members over the first 300 generated tokens. **(Right) Token-wise probability distributions of generated tokens at indices 700 to 1000:** we compare the distribution of token-wise probability between members and non-members over generated tokens at indices 700 to 1000.

1080 C.2 EXPERIMENTAL RESULTS
1081

1082 In this subsection, we report the additional experimental results. Here, these results are consistent
1083 with the conclusions drawn in the main text. Table 6 reports the TPR@1%FPR of our method and
1084 baselines on diverse distilled reasoning models. The results show that our method is effective on
1085 various dataset across three different models. Table 7 show the AUC and TPR@1%FPR scores
1086 of our method and baseline across various models. The experimental results demonstrate that our
1087 method is model-agnostic. Table 8 shows the AUC scores of our method and baselines on the S1
1088 dataset across three distinct settings. The results indicate the effectiveness of our method in settings
1089 where only the question, or the question along with the reasoning trajectories, is available.

1090 Table 6: TPR@1%FPR of our method and baselines on diverse distilled models. These models are
1091 produced through fine-tuning diverse different-sized models (e.g., Qwen2.5-32B-Instruct) on vari-
1092 ous distillation datasets, including S1, LIMO and S1.1 datasets. \dagger indicates methods that compute
1093 score using output tokens. **Bold** shows the superior result.

Method	Qwen2.5-7B-Instruct			Qwen2.5-14B-Instruct			Qwen2.5-32B-Instruct		
	S1	LIMO	S1.1	S1	LIMO	S1.1	S1	LIMO	S1.1
<i>Input-token-based methods</i>									
Perplexity (Li, 2023)	0.040	0.000	0.005	0.015	0.012	0.005	0.015	0.006	0.000
Lowercase (Carlini et al., 2021)	0.020	0.006	0.010	0.015	0.037	0.000	0.000	0.000	0.000
Zlib (Carlini et al., 2021)	0.025	0.000	0.000	0.015	0.006	0.000	0.005	0.000	0.000
Neighbor (Mattern et al., 2023)	0.025	0.018	0.005	0.030	0.006	0.005	0.025	0.012	0.005
MIN-K% (Shi et al., 2024)	0.040	0.000	0.005	0.010	0.012	0.010	0.015	0.006	0.000
MIN-K%++ (Zhang et al., 2025b)	0.040	0.018	0.025	0.000	0.024	0.010	0.025	0.006	0.000
Infilling Score (Raoof et al., 2025)	0.010	0.006	0.015	0.020	0.000	0.045	0.025	0.018	0.000
<i>Output-token-based methods</i>									
Generated Perplexity \dagger	0.235	0.128	0.070	0.350	0.171	0.045	0.160	0.226	0.080
Generated MIN-K% \dagger	0.235	0.128	0.070	0.350	0.171	0.045	0.160	0.226	0.080
Ours \dagger	0.345	0.256	0.095	0.375	0.226	0.090	0.470	0.335	0.110

1111 Table 7: AUC and TPR@1%FPR scores of our method and baselines on S1 dataset across various
1112 models, including Llama-3.1-8B- Instruct, Gemma-7B-it and Mistral-7B-Instruct-v0 models. **Bold**
1113 shows the superior result.

Method	AUC			TPR@1%FPR		
	Llama-3.1-8B	Gemma-7b	Mistral-7B	Llama-3.1-8B	Gemma-7b	Mistral-7B
Perplexity (Li, 2023)	0.529	0.537	0.549	0.015	0.015	0.005
Lowercase (Carlini et al., 2021)	0.524	0.537	0.486	0.005	0.005	0.025
Zlib (Carlini et al., 2021)	0.539	0.533	0.547	0.020	0.025	0.010
MIN-K% (Shi et al., 2024)	0.554	0.535	0.564	0.015	0.015	0.000
MIN-K%++ (Zhang et al., 2025b)	0.562	0.532	0.543	0.005	0.010	0.005
Ours	0.927	0.943	0.953	0.365	0.400	0.220

1126 D USE OF LARGE LANGUAGE MODELS
1127

1128 This paper utilizes large language models solely for the purpose of enhancing the clarity and pre-
1129 cision of specific sentences, without further use of LLMs for additional purposes.

1134
 1135
 1136
 1137
 1138
 1139
 1140
 1141
 1142
 1143
 1144
 1145
 1146
 1147
 1148
 1149
 1150
 1151
 1152
 1153

1154 Table 8: AUC scores of our method and baselines on S1 dataset across three distinct settings: using
 1155 only the question (Question-Only), using the question along with the reasoning trajectories (Ques-
 1156 tion-CoT), and using the full sample (Question-CoT-Answer). **Bold** shows the superior result.

1157
 1158
 1159
 1160
 1161
 1162
 1163
 1164
 1165
 1166

Method	Question-Only	Question-CoT	Question-CoT-Answer
Perplexity (Li, 2023)	0.444	0.972	0.988
Lowercase (Carlini et al., 2021)	0.435	0.998	1.000
Zlib (Carlini et al., 2021)	0.474	0.940	0.966
MIN-K% (Shi et al., 2024)	0.443	0.972	0.988
MIN-K%++ (Zhang et al., 2025b)	0.472	0.704	0.723
Ours	0.855	0.872	0.872

1167
 1168
 1169
 1170
 1171
 1172
 1173
 1174
 1175
 1176
 1177
 1178
 1179
 1180
 1181
 1182
 1183
 1184
 1185
 1186
 1187